Proceedings of 15th International Marine Design Conference (IMDC-2024)
June 2-6, 2024
Amsterdam, the Netherlands

A comparative analysis of side and stern installation of a monopile lifting operation using a heavy lift crane vessel

A.M. Elzinga [1,2,*], J.D. Stroo [2], and A.A. Kana [3]

ABSTRACT

This paper compares two 2XL monopile installation methods: at the leeward side of the heavy lift crane vessel and in the recess at the stern of the vessel. The multi-body system of the vessel, monopile, crane, and mission equipment induces interaction and resonance behaviour. Operational limits are assessed at the crane tip and pile gripper during upending and lowering of the monopile. Stern installation provides a larger operability window during upending compared to side installation. During the lowering stage, the operability depends on the monopile submergence: side and stern installation provide a comparable operability. Considering both stages, stern installation shows promising results.

KEY WORDS

Heavy lift vessel; monopile; installation method; allowable sea states; time-domain simulation

INTRODUCTION

The offshore wind energy sector is rapidly growing with an increase in the capacity of offshore wind turbines (OWT). This implies an increase in size and weight of OWTs. Additionally, there is a tendency to locate offshore wind farm sites further offshore. More consistent wind speeds, and therefore better quality wind resources, and more space are available further offshore. Sites with a water depth of less than 70 metres are suitable for OWT-fixed bottom foundations. The increasing capacity and greater water depth at OWF locations result in increasing OWT, and therefore also the foundation of the OWT (Ulstein, 2019). A commonly applied fixed-bottom foundation is the monopile. 65% of the fixed-bottom foundations worldwide are monopiles (MP). In the planning phase, 88% of the fixed-bottom foundations are monopiles, due to their simplicity, ease of installation, and relatively low costs (Inernational Energy Agency, 2019; Liu, 2021; Ramírez et al., 2020). Over the past years, the diameter of an MP, an indicator for its size and weight, increased from an average of 5 metres to 10-12 metres. Monopiles are categorised into L, XL, XXL (2XL), and XXXL (3XL) monopiles. 2XL monopiles have an average diameter of 10 metres and a weight of around 2500 tonnes (Stroo, 2023a).

Monopiles are typically installed from jack-up vessels, which provide a stable platform. However, these vessels are limited in terms of water depth, seabed conditions, and crane capacity. The ever-growing monopiles need to be installed from floating vessels, such as a heavy lift crane vessel (HLV). Heavy lift crane vessels are not dependent on the water depth, seabed conditions, or the crane capacity due to the absence of the extendable legs of a jack-up vessel. During installation, the heavy lift crane vessel forms a multi-body system with the crane and monopile, inducing coupled dynamic behaviour. Pendulum effects of the monopile might occur. The current method to install an MP from a heavy lift crane vessel is at the

[1] Department of Maritime and Transport Technology, Delft University of Technology, Delft, The Netherlands
[2] Ulstein Design & Solutions B.V., Rotterdam, The Netherlands
[3] Department of Maritime and Transport Technology, Delft University of Technology, Delft, The Nederlands; ORCID: 0000-0002-9600-8669
[*] Corresponding Author: anke.marij.elzinga@ulstein.com

Submitted: 8 March 2024, Revised: 27 April 2024, Accepted: 3 May 2024, Published: 16 May 2024

Conference paper, DOI: https://doi.org/10.59490/imdc.2024.822 e-ISSN: 3050-4864

leeward side of the vessel. The monopile is placed transversely on deck and upended to a vertical position at the starboard side of the vessel, after which it is lowered towards the seabed. The vessel creates a shielding effect. This method is called side installation. A new development is stern installation (Stroo, 2023b). The MP is placed longitudinally on deck and is upended in the centre line of the vessel. The lowering of the MP takes place in a recess at the stern of the vessel, creating a shielded environment. This principle can be compared to the installation concept of pipe layers.

The lowering stage of the monopile installation is considered as a critical event (Li et al., 2015; Guachamin-Acero et al., 2016; Chen et al., 2022). The multi-body system of the vessel, monopile, crane, and mission equipment induces interaction and resonance behaviour might occur. Therefore, it is important to assess the operational limits. Moreover, it is required to assess these limits during marine operations in the planning phase. The purpose of this paper is to present a comparison between side and stern installation using a heavy lift crane vessel during upending and lowering of an XXL monopile (2XL MP) in terms of operational limits.

METHOD & TOOLS

A general evaluation method is defined to establish the operational limits of an installation method, which can be applied parallel to multiple installation methods. Two different installation methods are evaluated for the same vessel and mission equipment. The design of the hull and mission equipment, such as the crane and pile gripper, are not a part of this study. Therefore, this evaluation method focuses on the effects of different installation methods on the dynamic behaviour of the coupled HLV-MP system.

The installation sequence of the method needs to be defined, where after the key positions of the sequence are established. The loading condition of every key position is calculated and the loading conditions are applied. The floating equilibrium needs to be found for every loading conditions. If realistic, the hydrodynamic properties of the loading condition are generated. The response at the relevant positions, obtained by numerical simulations, is analysed of which then the key critical positions are identified. The most critical positions may be reviewed again in more detail. The operational limits are obtained from the response, leading to a comparison between the two monopile installation methods. The method is presented in a flowchart in Figure 1. The loading conditions are based on existing loading conditions, generated in DELFTship. The applied loading conditions are calculated in Excel, which is also used for pre- and post-processing the results. HydroD, a diffraction programme, is used to calculate the load and displacement RAOs, added mass and damping matrices. The numerical time-domain simulations are performed in OrcaFlex, a package for dynamic analysis of offshore marine systems.

CASE STUDY

Hornsea Offshore Wind Farm on the North Sea is used as a reference project. Monopiles are installed at a water depth of 68 metres, the largest known water depth for MP installation, based on 4C Offshore data (2022). The environmental data is based on the wind and wave characteristics of the North Sea. The JONSWAP spectrum is applied as wave spectrum. For the wind speed spectrum, the NPD wind speed spectrum is applied. For side installation, the wave direction is 210° to create a shielding effect, according to the angle definition as defined in Figure 2. For stern installation, the wave direction is 180°. Wave spreading and current are excluded. Significant wave height, H_s, values of 2 and 3 metres are chosen. Figure 3 shows the seasonal mean H_s, with the upper red dot representing Hornsea Wind Farm. During spring and summer, a mean H_s of 1.5 metres is observed. During autumn and winter a mean H_s of 2.5 metres is observed.

The spectral peak period T_p is varied between 5.0 and 15.0 seconds, as presented in Table 1. This range is chosen based on wave scatter diagram, as presented in Figure 4, and the hindcast data of Hornsea Wind Farm. The shorter wave periods around 5.0 to 8.0 seconds occur more frequently on the North Sea, due to the relatively small water depth. However, the larger wave periods are included in the case study to assess the dynamic behaviour for these environmental conditions and to put the results of the shorter wave periods into perspective. Additionally, by simulating these larger wave periods on purpose, the critical conditions can be assessed.

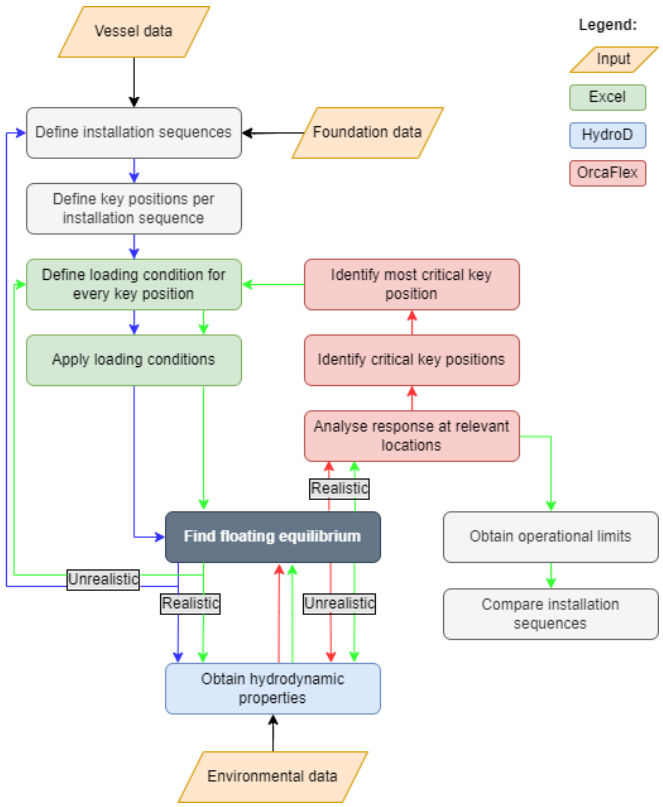

Figure 1: Flowchart of the applied method to establish the operational limits: from definition of installation sequences and loading conditions to analysis of responses at relevant locations and comparison of installation sequences.

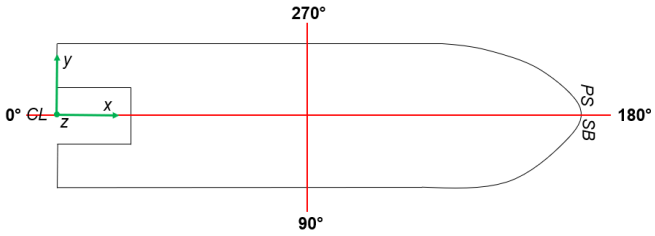

Figure 2: Angle definition for wave direction and slewing angle for the crane boom

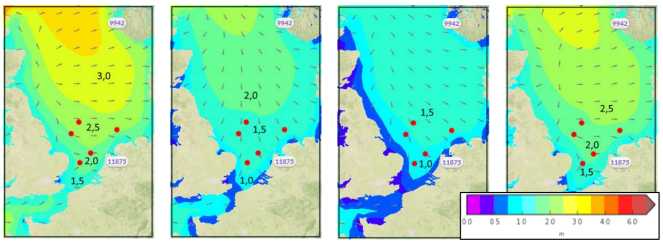

Figure 3: Seasonal mean H_s [m] in January - April - July - October on the North Sea with MetOcean View Hindcast (Brans et al., 2021; MetOcean Solutions, 2020)

Table 1: Range of simulated spectral peak period T_p [s]

T_p [s]	5.0	6.1	7.2	8.3	9.4	10.6	11.7	12.8	15.0

Percentage [%] of occurrence of joint significant wave height and zero up-crossing period for North Sea (zone 11)

Hs [m] \ Tp [s]	5,0	6,1	7,2	8,3	9,4	10,6	11,7	12,8	15,0	Sum [%]
Tz [s]	3,9	4,7	5,6	6,5	7,3	8,2	9,1	10,0	11,7	
0	0,00	0,00	0,00	0,00	0,00	0,00	0,00	0,00	0,00	0,00
1	6,69	12,65	10,53	5,37	2,01	0,55	0,15	0,04	0,00	37,98
2	1,23	5,05	7,86	6,76	3,95	1,65	0,62	0,21	0,02	27,35
3	0,21	1,48	3,59	4,44	3,53	1,97	0,93	0,38	0,05	16,57
4	0,03	0,38	1,33	2,21	2,25	1,58	0,89	0,43	0,07	9,16
5	0,01	0,09	0,43	0,93	1,18	1,00	0,66	0,36	0,07	4,74
6	0,00	0,02	0,13	0,35	0,54	0,55	0,42	0,26	0,06	2,32
7	0,00	0,00	0,04	0,12	0,22	0,27	0,23	0,16	0,05	1,09
8	0,00	0,00	0,01	0,04	0,08	0,12	0,12	0,09	0,03	0,49
9	0,00	0,00	0,00	0,01	0,03	0,05	0,05	0,05	0,02	0,21
10	0,00	0,00	0,00	0,00	0,01	0,02	0,02	0,02	0,01	0,09
Sum [%]	8,17	19,67	23,92	20,22	13,81	7,75	4,08	1,98	0,39	100,00

Figure 4: Wave scatter diagram based on empirical data of the North Sea (zone 11) (DNV, 2021a)

The multi-body system consists of a vessel, monopile, crane, and pile gripper ring. The reference vessel is a heavy lift crane vessel developed by Ulstein, HX118, with a recess in the stern for both side and stern installation. The characteristics are presented in Table 2. The monopile is a 2XL monopile (Table 3). The mission equipment consists of a crane and a pile gripper ring, which is acting as a hinge. The mass moments of inertia of the crane boom and pile gripper ring are calculated using thick-walled theory of a cylinder. This complete multi-body system is visualised in Figure 5.

Table 2: Characteristics of heavy lift crane vessel

Characteristics	*HX118*
Length [m]	215.60
Beam [m]	57.40
Depth [m]	16.80
Max. deadweight [tonnes]	40000

Table 3: 2XL monopile characteristics

Characteristics	*2XL MP*
Length [m]	100
Diameter [m]	11
Mass [tonnes]	2300

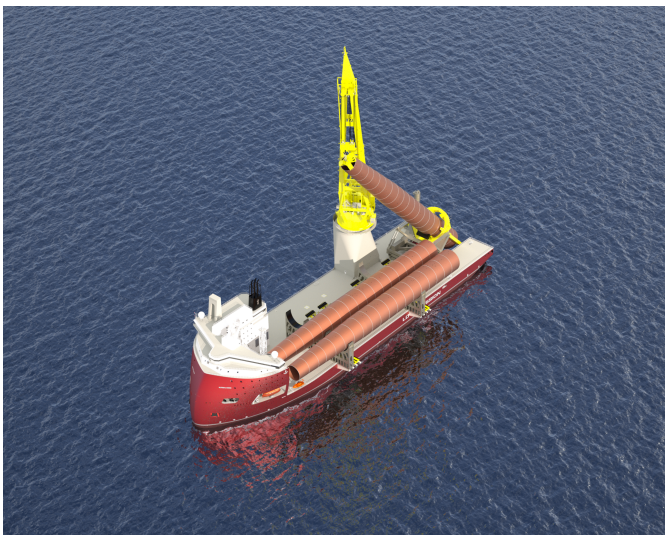

Figure 5: HX118 upending an MP in the stern

MODELLING OF COUPLED HLV-MP SYSTEM

This section discusses the modelling of the case study. The loading conditions for both installation methods are covered. Additionally, the modelling of the input data in OrcaFlex is presented, together with the used simulation approach.

Installation sequence

The upending and lowering process for side installation is schematically represented in Figure 6. Five loading conditions are set up: the monopile in horizontal position, the monopile 45° upended, a fully upended monopile, the monopile halfway the water depth (35 metres of submergence), and finally the monopile 3 metres above seabed (65 metres of submergence). The upper part of the monopile is guided by the crane. The lower end of the monopile is placed into the pile gripper, which acts as a hinge, and upending frame. The upending frame prevents the monopile from sliding through the gripper. After upending, the upending frame is removed by rotating 90°. When the monopile is fully upended, the monopile is still in the frame of the pile gripper ring. This results in a level of submergence of 5.56 metres. The pile gripper is lowered towards the water surface, the bottom support is opened and then the monopile is lowered.

The loading conditions corresponding to each stage of the installation sequence are established and are presented for side and stern installation in Table 4. The loading condition depends on the position of the monopile, and is defined for the stages depicted in Figure 6. The coding *GE-03-80%* stands for general departure empty, consumable tanks filled at 80%. *LI* implies a lifting condition with the main crane. The load is 2300 tonnes, at a certain radius from the centre of rotation of the crane in the horizontal plane. The lightship weight and deadweight are based on the loading conditions of the reference vessel HX118. The inertia terms are simplified by only taking the Steiner terms into account. The buoyancy of the partly submerged monopile is also excluded. The luffing and slewing angle are calculated based on the angle convention as depicted in Figure 2. The transverse centre of gravity (TCG) and longitudinal centre of gravity (LCG) are set to have zero list and trim by using a nonlinear solver varying the water ballast (and anti-heeling tanks). This nonlinear solver is a Generalised Reduced algorithm, which is an extension of the simplex method for linear programming (Lasdon et al., 1978). The corresponding vertical centre of gravity (VCG) and free surface moment (FSM) are calculated, based on International Maritime Organization (IMO) rules (International Maritime Organization, 2022).

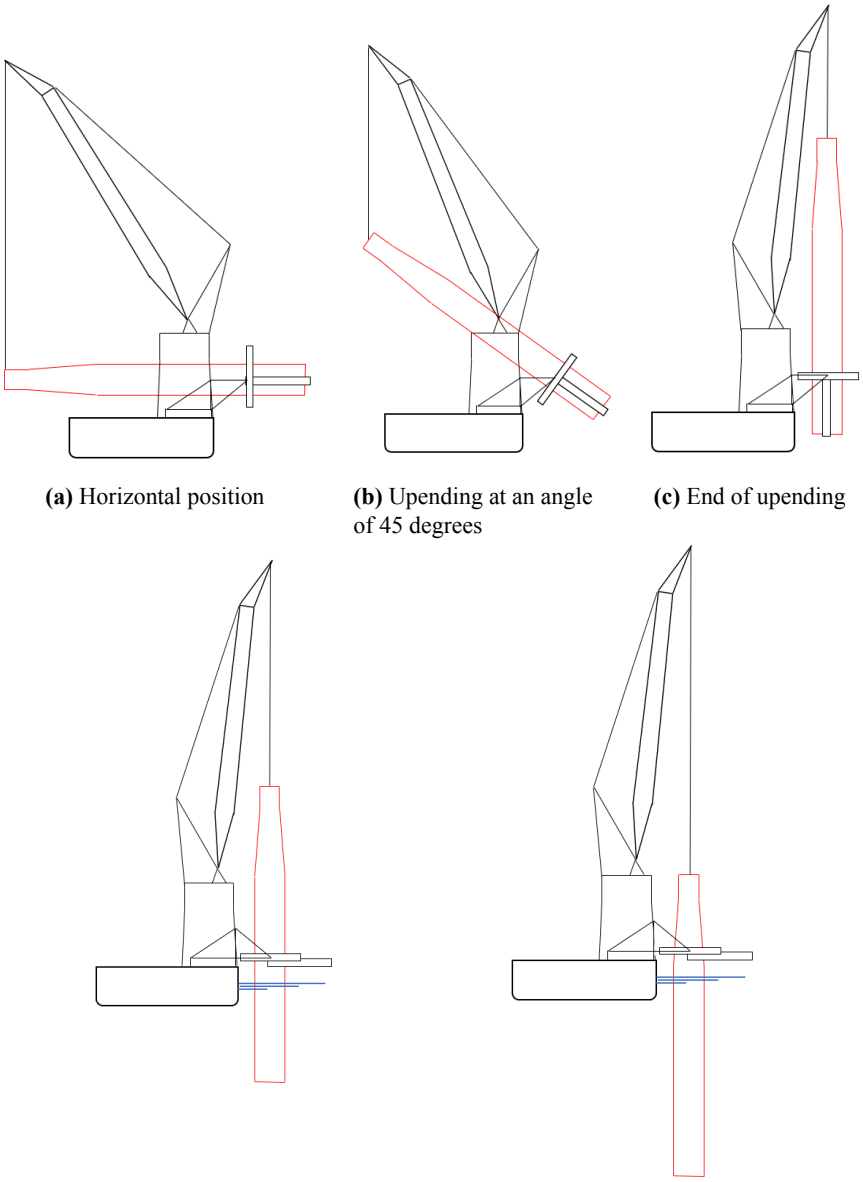

(a) Horizontal position

(b) Upending at an angle of 45 degrees

(c) End of upending

(d) 35 metres of submergence

(e) 65 metres of submergence

Figure 6: Stages of upending and lowering of a monopile towards the seabed for side installation

The installation sequence of stern installation is similar to side installation. The schematic representation of stern installation is depicted in Figure 7. The crane is at the same position as for the side installation. The pile gripper is placed at the centre line of the vessel in front of the recess. The monopile is upended in the centre line of the vessel in a similar way as pipe-laying vessels. Stern installation provides a sheltered installation position. The loading conditions for stern installation (Table 4) are established similarly to the loading conditions of side installation.

Table 4: Loading conditions for side and stern installation

	Position MP	Side installation	Stern installation
1	Horizontal position	GE-03-80%-LI: 2300t@63.8m, 243°	GE-03-80%-LI: 2300t@63.8m, 221°
2	45° upended	GE-03-80%-LI: 2300t@50.7m, 235°	GE-03-80%-LI: 2300t@27.9m, 247°
3	Fully upended	GE-03-80%-LI: 2300t@31.6m, 159°	GE-03-80%-LI:2300t@47.8m, 303°
4	Halfway water depth	GE-03-80%-LI: 2300t@31.6m, 159°	GE-03-80%-LI:2300t@47.8m, 303°
5	3 metres above seabed	GE-03-80%-LI: 2300t@31.6m, 159°	GE-03-80%-LI:2300t@47.8m, 303°

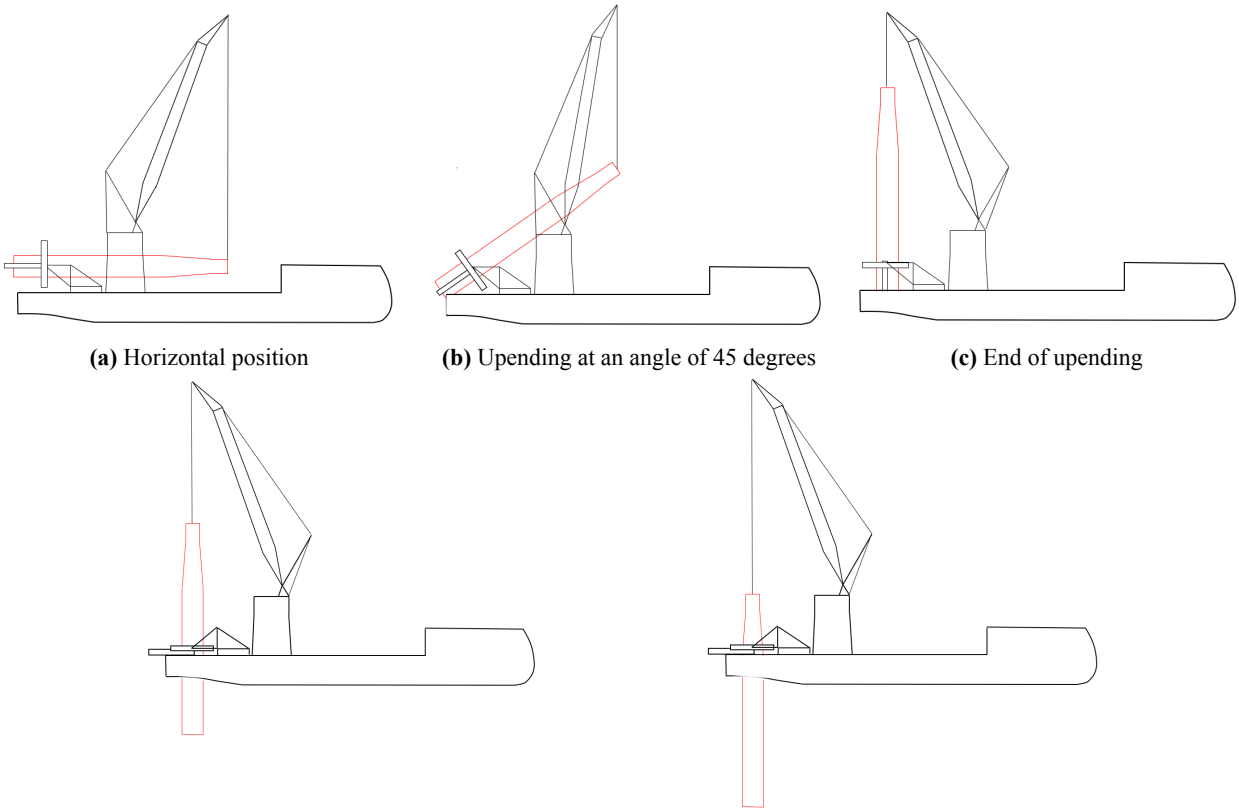

(a) Horizontal position **(b)** Upending at an angle of 45 degrees **(c)** End of upending

(d) 35 metres of submergence **(e)** 65 metres of submergence

Figure 7: Stages of upending and lowering of a monopile towards the seabed for stern installation

OrcaFlex model

The installation sequences including the generated hydrodynamic properties are set up in OrcaFlex. The multi-body system is modelled identically for side and stern installation except for the location of the monopile and pile gripper ring. The properties of the vessel, mission equipment and monopile are identical as well. This section describes the important modelling choices regarding the monopile, mission equipment, wave shielding, and simulation approach. Based on this model set-up, time-domain simulations are performed.

Monopile

Depending on the position of the MP, the MP is modelled differently to incorporate all the relevant hydrodynamic information. When the MP does not have any water contact, the monopile is modelled as a line object, as presented in Figure 8. A line is a flexible linear element in OrcaFlex which can be used for ropes, chains, but monopiles as well. The chosen line type is a general pipe with the inner and outer diameter and structural properties inserted as defined in Table 3. When the MP is (partly) submerged, the monopile is modelled as a hybrid buoy-vessel-line object. The spar buoy accounts for the viscous drag and inertia regime, while the vessel accounts for the diffraction regime. The vessel object also includes the tip vortex damping derived from model tests and CFD tests in a cooperation with Ulstein Design & Solutions, Huisman Equipment and Heerema. The vessel object is part of a multi-body group, together with the vessel itself. This multi-body group allows interaction between these two objects, such as wave shielding. Additionally, the multi-body group defines properties such as the frequency dependent added mass and damping matrices of the monopile and the vessel, and the hydrostatic stiffness are also defined in this multi-body group. The line object acts as a sleeve and models the contact with the pile gripper ring. The vessel and line object are rigidly connected to the 6 DoF spar buoy. The hybrid modelling for the submerged monopile is shown in Figure 9.

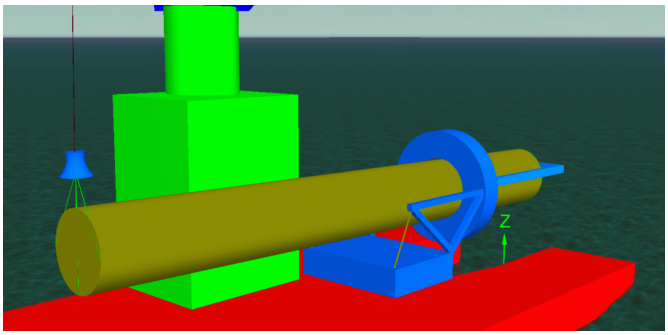

Figure 8: Modelling of monopile in OrcaFlex as line object for horizontal and upended monopile

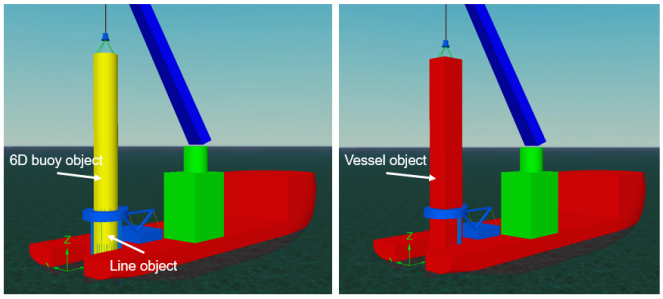

Figure 9: Modelling of monopile in OrcaFlex as hybrid buoy-vessel-line object for partly submerged monopile

The spar buoy creates the possibility to include the corresponding drag coefficient, added mass, slamming coefficients, and more accurately the buoyancy force. The spar buoy is discretised into multiple cylinders to better control the buoyancy force. The hydrodynamic loads on spar buoys are calculated with Morison's equation (Morison et al., 1950). The added mass and drag forces are applied on the submerged parts. When the object is partly submerged, the forces are scaled to the proportion of cylinder volume of the submerged buoy. The interaction effects on the fluid forces between the vessel and the monopile are imported from HydroD. A special multi-body group is created to take these effects into account.

The Morison equation for a fixed object in an oscillatory flow is shown in Equation 1. The first addend represents the fluid inertia force, related to the water particle acceleration, while the second addend represents the drag force, related to the water particle velocity. For a cylinder with a diameter D Equation 1 is rewritten to Equation 2.

$$F = \rho \cdot C_m \cdot V \cdot \dot{u} + \frac{1}{2} \cdot \rho \cdot C_d \cdot A \cdot u \cdot |u| \tag{1}$$

$$F = \rho \cdot C_m \cdot \frac{\pi}{4} \cdot D^2 \cdot \dot{u} + \frac{1}{2} \cdot \rho \cdot C_d \cdot D \cdot u \cdot |u| \tag{2}$$

When the object itself also moves with a velocity $v(t)$, the Morison equation is rewritten to an equation with three addends. (Equation 3): respectively the Froude-Krylov force, which is proportional to the fluid acceleration relative to the earth, the hydrodynamic added mass force, which is proportional to the fluid acceleration relative to the body, and lastly the drag force:

$$F = \rho \cdot V \cdot \dot{u} + \rho \cdot C_a \cdot V \cdot (\dot{u} - \dot{v}) + \frac{1}{2} \cdot \rho \cdot C_d \cdot A \cdot (u - v)|u - v| \tag{3}$$

Mission equipment

The crane consists of a slewing column and a crane boom. The slewing column rotates, however the vertical position remains identical. Therefore, the slewing column is not separately modelled in terms of mass and mass moment of inertia, but included in the vessels mass and inertia. The crane boom however changes in the x, y, and z direction which affects the mass moment of inertia and the loading condition. The crane boom and crane hook are separately modelled. The crane hook is connected to the monopile with 4 springs. The crane hook has 6 degrees of freedom to model the behaviour of the crane hook as realistic as possible.

Wave shielding

Wave shielding is a phenomenon of diffraction of the incoming waves by the presence of a hull or object. For side installation, the monopile is lowered at the leeward side of the vessel. For stern installation, the monopile is lowered in the recess of the stern. The position and behaviour of the monopile is influenced by the presence of the vessel. The wave shielding reduces the overall dynamic forces that act on the subsea asset when it is lowered due to the decrease of the displacement, velocity and acceleration of the waves (Li et al., 2014; Amer et al., 2022). It is modelled in OrcaFlex by sea state RAOs defined for vessel objects in multi-body groups. These RAOs depend on the wave direction, wave frequency, velocity potential and velocity potential gradient, and are generated in HydroD. Shorter waves are more affected by shielding, because the vessel tends to follow the motion for longer waves. The hull of the vessel and the vessel object of the monopile are modelled in a multi-body group which allows to account for the interaction between these two objects, and therefore for wave shielding.

A comparison of the monopile force is made between CFD tests and the OrcaFlex simulations. The CFD tests are performed internally at Ulstein, for a wave height of 4.65 metres, corresponding with the highest wave height for H_s of 3 metres, and a wave period of 7.0 seconds, using Airy wave theory (Stroo, 2022). The water depth is 50 metres and the monopile of 100 metres is fixed at the seabed. The wave direction is 210° for side installation. For stern installation, the wave direction is 165°. The MP force for side and stern installation is divided by the MP force without the presence of a vessel. The wave height, wave period and wave direction of the CFD tests are implemented in the OrcaFlex files to enable a comparison. The loading condition of the monopile 3 metres above seabed is used as a basis. Between the CFD and OrcaFlex are multiple modelling differences: the position of the monopile is slightly different for side and stern installation, the loading conditions are not identical, and diameter of the MP is 10 metres for the CFD tests and 11 metres for the OrcaFlex simulations. The results between the two methods are presented in Table 5.

Table 5: Comparison between maximum horizontal force for CFD tests and OrcaFlex simulations for side and stern installation, with a wave direction of respectively 210° and 165° with a wave height of 4.65 metres and wave period of 7 seconds

	CFD	OrcaFlex
$\frac{F_{MP_{stern}}}{F_{MP}}$ [%]	24%	31%
$\frac{F_{MP_{side}}}{F_{MP}}$ [%]	33%	35%
$\frac{F_{MP_{stern}}}{F_{MP_{side}}}$ [%]	74 %	89 %

The results for side installation for the CFD tests and OrcaFlex correspond, with a difference of 2 %. The differences in results for stern installation are larger, due to difference in modelling the recess for the CFD tests and OrcaFlex. The sea state RAOs of OrcaFlex are generated in HydroD, which cannot deal with the sides of the recess. This leads to the difference in MP forces for stern installation. A more accurate modelling of the recess in HydroD will probably provide a larger reduction in MP force and larger shielding effect for the OrcaFlex simulations.

Simulation approach

The upending and lowering of a monopile is a nonstationary process. Two approaches to simulate nonstationary processes are proposed by Sandvik (2012):

1. Steady-state simulations in irregular waves of the most critical vertical positions of the object.
2. Simulations of a repeated nonstationary lowering process with different irregular wave realisations and for every simulation an analysis of the extreme response.

It was shown that the second approach, to have a repeated nonstationary lowering process, results in more realistic results compared to the steady-state simulations. The first approach creates a build-up of oscillation which is not observed in reality. However, steady-state simulations in the time domain are applied due its relatively fast, effective and simple way of modelling an installation sequence, compared to modelling a nonstationary version of the same installation sequence. By simulating different loading conditions of the installation sequence for various environmental conditions, the critical situations for different T_p and H_s can still be distinguished. For further research, setting up simulations with a nonstationary lowering process are recommended and interesting to analyse differences between the steady-state simulations and repeated nonstationary lowering processes.

The duration of the simulation is set at 1800 seconds, which is found to be a sufficient representative of a sea state reference period, which is 3 hours. Besides the actual simulation time of 1800 seconds, a build-up period of 50 seconds is applied, which provides a smooth build-up of sea conditions to avoid transients when the simulation starts.

Due to the stability, the implicit time integration method is applied with a constant time step. A time step sensitivity analysis is conducted for 0.01, 0.10, and 1.00 seconds, as presented in Figure 10a, Figure 10b, and Figure 10c. A trade-off between capturing all the relevant effects and the computational time led to a time step of 0.1 seconds. A larger time step results in less computational time, however the difference in results between 0.01 and 0.10 seconds is found to be small enough. Therefore, a time step of 0.1 seconds is found to be sufficient.

A sea state reference period takes 3 hours. For the numerical simulations a simulation time of 1800 seconds is set. In Figure 11a, Figure 11b, and Figure 11c, a comparison between a simulation time of 1800 seconds and 3 hours are displayed for the loading condition where the MP is submerged for 5.56 metres, with a H_s of 2 metres and a T_p of 12.8 seconds. The total energy of the 3 hours run seems slightly higher for the dynamic x and y than for the 1800 seconds run. In addition, for the dynamic x and y, there are some differences in the curve of the graph due to possibly more scatter of waves, which are

or are not in the simulation. For the dynamic y, the natural frequency of the MP seems more dominant, which explains the better correspondence compared to the dynamic x. In conclusion, the differences in spectral density are found to be negligible enough to continue with the 1800 seconds simulation time while also taking into account the longer computational time which is needed for 3 hours simulations.

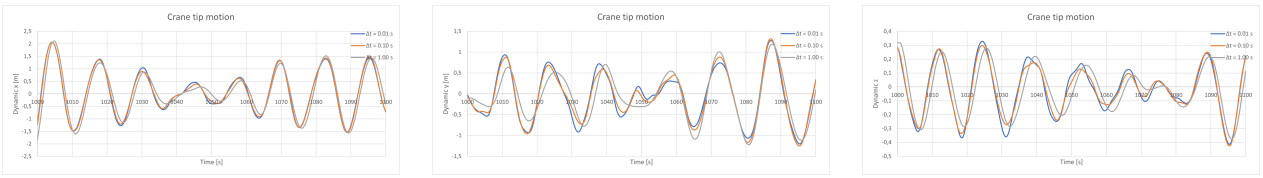

(a) Dynamic x [m] **(b)** Dynamic y [m] **(c)** Dynamic z [m]

Figure 10: Dynamic x, y, and z at the crane tip [m]

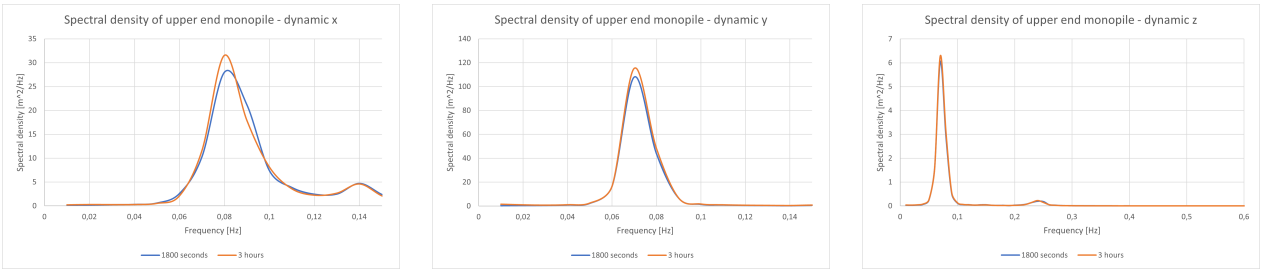

(a) Dynamic x [m] **(b)** Dynamic y [m] **(c)** Dynamic z [m]

Figure 11: Dynamic x, y, and z at the monopile tip [m]

DOUBLE PENDULUM CALCULATIONS

The multi-body behaviour of the crane boom with the monopile, rigging and crane hook results in resonance behaviour when the peak period of the wave coincides with the natural periods of system. The eigenfrequencies are determined to explain behaviour observed in the results. The natural periods are analytically derived for a double pendulum. The double pendulum includes the characteristics of the falls, crane hook, and 2XL monopile, but neglects the presence of the pile gripper ring. A schematic representation is presented in Figure 12.

For the double pendulum, there are two angles of inclination, θ_1 and θ_2. The small angle approximation is also applied for the double pendulum. The equation of motion is solved with the assumption that the solution is a sine-function. This results in Equation 4, which is an eigenvalue problem with two degrees of freedom.

$$\mathbf{K} \cdot \mathbf{x} = \lambda \mathbf{M} \cdot \mathbf{x} \tag{4}$$

The natural periods are calculated for multiple levels of MP submergence and graphically displayed in Figure 13. The two natural periods of the monopile do not coincide between 0 and 65 metres of MP submergence. The first and second natural period flip between 15 and 20 metres of submergence, because the natural period of the falls and the monopile, and therefore the rotation point, change over a different submergence levels. The difference between the natural periods increases when the monopile is more submerged.

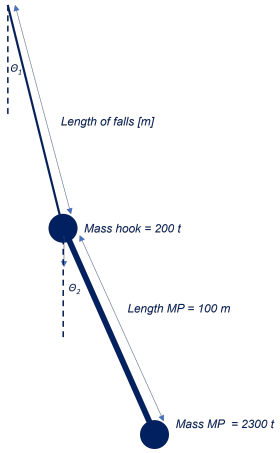

Figure 12: Schematic representation of the double pendulum with the characteristics of the falls, the crane hook, and the 2XL MP without the pile gripper ring

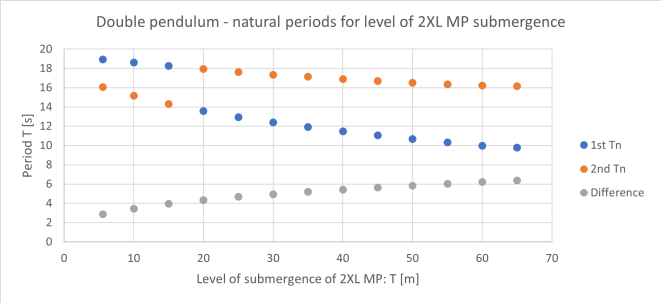

Figure 13: Natural periods for multiple levels of submergence of the monopile

The double pendulum calculations include the added mass. When the monopile is more submerged, the added mass is larger. The rotation point shifts downwards, and the added mass shifts upwards over the length of the monopile (Dam, 2018). These shifts reduce the distance between these two points and therefore reduces the inertia moment. The influence of the reduced arm is larger than the increase in added mass, since the length is squared. Therefore, the mass matrix reduces, resulting in a decrease in natural period. This effect corresponds with the results of the double pendulum calculation.

NATURAL PERIODS HLV & MP

The natural periods of the vessel and the monopile are relevant for the analysis of the operational limits. The natural periods for the vessel for heave, roll, and pitch for side and stern installation are presented in Table 6. These periods are obtained from the vessel RAOs generated in HydroD. The natural periods for the MP for sway, heave, and roll are shown in Table 7.

Table 6: Natural periods of the vessel for side and stern installation, based on vessel RAOs depending on corresponding wave direction

HLV	**Heave**	**Roll**	**Pitch**
Side installation	13 s	13 s	13 s
Stern installation	14 s	-	14 s

Table 7: Natural periods of MP, based on MP RAOs, for fully upended MP

MP	Sway	Heave	Roll
	6 s	6 s	6 s

OPERATIONAL LIMITS

The operational limits are considered for the mission equipment, and are based on the following key indicators:

- Off- and sidelead at the crane tip in vessel x- and y-direction
- Dynamic amplification factor of the crane
- Dynamic utilisation factor of the crane
- Dynamic utilisation factor of the interface loads at the pile gripper ring in global x- and y-direction

The results for side and stern installation expressed in terms of these key indicators.

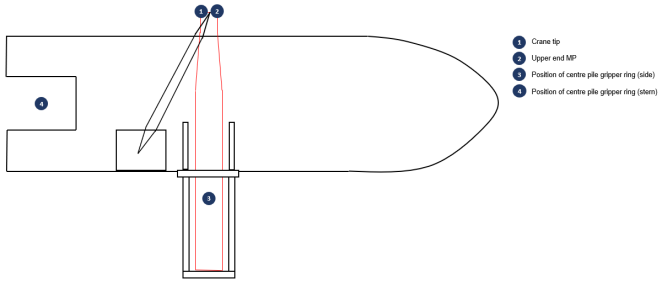

Figure 14: Locations for response analysis with the position of the pile gripper ring at starboard of the vessel for side installation and at the recess for stern installation

Crane tip forces

The crane tip forces in x, y-, and z-direction in the global coordinate system are necessary to obtain the operational limits in terms of a off- and sidelead at the crane tip, and the dynamic amplification factor (DAF) and dynamic utilisation factor (DUF) of the crane tip. The off- and sidelead are calculated with respectively F_x and F_y of the global coordinate system. The DAF and DUF are assessed using F_z of the global coordinate system.

Off- and sidelead

The sidelead (ϕ_{crane}) and offlead (θ_{crane}) at the crane tip are the maximum allowable angles when hoisting or lifting a load, and are defined based on the global coordinate system of the vessel. The maximum values of the off- and sidelead are provided by the manufacturer of the crane.

The sidelead of a crane consists of a static and dynamic part. The static sidelead is the heeling of the crane. The dynamic part of the sidelead is the dynamic angle between the vertical and the hoist tackle, resulting from swinging of the lifted load due to slewing and/ or drift-off of the vessel (Huisman, 2021).

Similarly the offlead consists of a static and dynamic part. The static offlead is the trim of the crane. It is the angle between the crane slewing axis and vertical, as a result of the static inclination of the vessel, and is in plane of the boom. The dynamic offlead is the dynamic angle between the vertical and the hoist tackle, as a result of swinging of the lifted load due to slewing and/or drift-off of the vessel, which is in plane of the boom (Huisman, 2021).

For the crane with a maximum capacity of 5000 tonnes at a radius of 36 metres in horizontal plane, used in this case study, both the off- and sidelead have a maximum angle of 3.5°, including a maximum of 1° from the crane heel or trim, as provided by the crane manufacturer. For this crane capacity condition, the off- and sidelead are equal. Therefore, the maximum off- and sidelead at the crane tip are also set to 3.5°.

From the F_x and F_y of the crane tip, the off- and sidelead are calculated to check whether the maximum limit is exceeded as presented in Equation 5 and Equation 6.

$$\phi_{crane} = \arctan(\frac{F_y}{(M_{MP} + M_{rigging}) \cdot g}) \tag{5}$$

$$\theta_{crane} = \arctan(\frac{F_x}{(M_{MP} + M_{rigging}) \cdot g}) \tag{6}$$

Dynamic Amplification Factor (DAF)

The DAF is a dimensionless ratio representing the dynamic hook load at the crane tip to its static hook force as described in Equation 7 and Equation 8.

$$DAF = \frac{Dynamic\ hook\ load}{Static\ hook\ load} \tag{7}$$

$$Static\ hook\ load = (M_{MP} + M_{rigging}) \cdot g \tag{8}$$

DAF is used for lifting operations to account for global dynamic effects (DNV, 2021b). This DAF should be determined by either specific analysis of the operation or by model testing. Depending on the location of the operation and the static hook load (SHL), the factor varies: offshore operations require higher DAFs compared to inshore or onshore, and for larger static hook loads the DAF becomes less. For this offshore marine operation with a 2XL MP, the maximum DAF is 1.15 based on the regulations of DNV (DNV, 2021b).

Dynamic Utilisation Factor (DUF)

The DUF is the dimensionless ratio between the dynamic vertical force on the crane tip and the maximum crane capacity as presented in Equation 9. This factor is introduced due to cases when the mass of the lifted load is relatively low compared to the crane capacity, but the DAF is already close to its maximum allowable limit. The DUF derived from the vertical dynamic crane tip force needs to be less than 1.00. The DUF is internally used at Ulstein and not described in literature.

$$DUF = \frac{Dynamic\ hook\ load}{Crane\ capacity \cdot g} \tag{9}$$

Pile gripper interface loads

The interface loads between the monopile and the pile gripper ring are considered as well. The pile gripper ring used for heavy lift crane vessels is specialised construction equipment. Therefore, there are no explicit regulations according to a class society like DNV. A DUF for the pile gripper ring is introduced in Equation 10 and Equation 11 to assess the lateral forces on the pile gripper ring. This DUF is the dimensionless ratio between the lateral force in the global coordinate system and the working load limit (WLL) in global x- and y-direction. The WLL for the pile gripper ring is not provided by the manufacturer for this case study, but a value is chosen based on the industry experience of Ulstein for global x- and y-direction.

$$DUF_{pile\ gripper\ ring\ x} = \frac{F_x}{WLL} \tag{10}$$

$$DUF_{pile\ gripper\ ring\ y} = \frac{F_y}{WLL} \tag{11}$$

The DUF for the pile gripper is only applied when the MP is lowered. During the upending of the monopile, the pile gripper ring is not acting as a gripper. The mass of the MP is then divided between the crane and a steel cradle with a rubber pad on which the MP partly rests. This implies the DUF to be irrelevant for the loading conditions during the upending of the monopiles.

RESULTS

The results are presented per key indicator and H_s. The key indicators are calculated based on crane tip forces and pile gripper contact forces, which are the Most Probable Maximum (MPM) for each T_p. The MPM is an extreme value statistic, based on the Rayleigh distribution. In Table 9, Table 8, and Table 10 an overview is presented for which loading conditions the maximum allowable limits are exceeded.

Side installation

In Table 8 and Table 9 an overview of the operability per loading condition of the upended and lowered MP is presented for side installation for a range of T_p between 5.0 and 15.0 seconds. A checkmark implies that that specific operational limit based on the MPM of the crane tip force or pile gripper force is not exceeded for the entire range of simulated T_p. When the allowable limit is exceeded, the corresponding spectral peak period is mentioned.

In Table 8 the operability check for the upending stage is presented, solely for the crane tip, for the horizontal position of the MP and the MP $45°$ upended for side installation. The offlead is limiting for side installation for the horizontally placed and $45°$ upended 2XL MP. For the horizontally placed MP, the vessel RAOs experience a maximum around the range of $12 - 15$ seconds. These maxima correspond with the maxima of the responses of the offlead. For the 45° upended MP, the sidelead is additionally exceeded at 15.0 seconds for side installation.

Based on Table 9, it is observed that the offlead, θ_{crane}, is limiting the operability. For the fully upended MP, the limits for the offlead is only exceeded at a T_p of 7.2 and 8.3 seconds. For the MP halfway the water depth, the offlead is first limiting and afterwards the pile gripper loads in x-direction, the DAF of the crane tip and finally the sidelead for H_s = 3 m. For T_p of 15.0 seconds for H_s of 3 metres, the DUF of the pile gripper in y-direction is exceeded. When the MP is 3 metres above the seabed, the allowable limits are not exceeded.

Table 8: Operability with a maximum off- and sidelead of 3.5 °, maximum crane tip DAF of 1.15, and crane tip DUF of 1 for range of T_p between 5.0 and 15.0 seconds for a horizontal placed and 45° upended 2XL MP for side installation and stern installation

Crane tip	H_s = 2 m	H_s = 3 m	H_s = 2 m	H_s = 3 m	H_s = 2 m	H_s = 3 m	H_s = 2 m	H_s = 3 m
	Side installation		*Side installation*		*Stern installation*		*Stern installation*	
	Horizontal position		*45° upended*		*Horizontal position*		*45° upended*	
Sidelead [°]	✓	✓	At 15.0 s	At 15.0 s	✓	✓	✓	At 12.8 s
Offlead [°]	>10.6 s	>10.6 s	>11.7 s	>10.6 s	✓	✓	✓	✓
DAF [-]	✓	✓	✓	✓	✓	✓	✓	✓
DUF [-]	✓	✓	✓	✓	✓	✓	✓	✓

For the fully upended monopile, the natural periods of the double pendulum calculation of Figure 13 are approximately 16 and 19 seconds. These values do not correspond with the displacement RAOs of the vessel for heave, pitch, and roll which peak around the 13 seconds. The MP halfway the water depth experiences the largest responses for peak periods larger than 8.3 with in general a maximum response at 12.8 or 15.0 seconds. This corresponds with the natural period based on the double pendulum calculations in Figure 13, based on the level of submergence of the 2XL MP. In addition, the displacement RAOs of the vessel for heave, pitch, and roll peak around the period of 12.8 seconds. The RAOs and the natural period of the double pendulum reinforce the responses, thus the analysed forces, which eventually result in a peak in the operational limits. Lastly, it is important to consider that these long waves do not occur regularly on the North Sea based on the wave scatter diagram in Figure 4. When the monopile is almost at the seabed, the responses are below the allowable limits. The natural periods of the double pendulum of the rigging and 2XL MP are outside the range of the peak of the displacement RAOs of the vessel. The motion behaviour of the monopile is damped by the wave loads. The responses due to behaviour of the multi-body system do not exceed the operational limits.

Table 9: Operability with a maximum off- and sidelead of 3.5°, maximum crane tip DAF of 1.15, crane tip DUF of 1 and pile gripper DUF for x- and y-direction of 1 for range of T_p between 5.0 and 15.0 seconds for a fully upended 2XL MP, a 2XL MP halfway the water depth, and 2XL MP 3 metres above seabed for side installation

Side installation		H_s = 2 m	H_s = 3 m	H_s = 2 m	H_s = 3 m	H_s = 2 m	H_s = 3 m
		Fully upended		*Halfway water depth*		*3 m above seabed*	
Crane tip	Sidelead [°]	✓	✓	At 12.8 s	> 10.6 s	✓	✓
	Offlead [°]	✓	At 7.2, 8.3 s	> 9.4 s	> 8.3 s	✓	✓
	DAF [-]	✓	✓	✓	≥ 10.6 s	✓	✓
	DUF [-]	✓	✓	✓	✓	✓	✓
Pile gripper	DUF_x [-]	✓	✓	> 10.6 s	> 9.4 s	✓	✓
	DUF_y [-]	✓	✓	✓	At 15.0 s	✓	✓

Stern installation

Table 8 also includes the operability for horizontal placed MP and the 45° upended monopile for stern installation. The offlead is not limiting the operability for stern installation for the horizontal placed MP and the MP 45° upended. The allowable limit for sidelead is exceeded at 12.8 seconds, for H_s of 3 metres, in case of the 45° upended monopile.

The operability overview of the lowering of the MP for stern installation is shown in Table 10. The allowable limits are similar to side installation. The offlead is governing the allowable limits for the lowering stage as it is first exceeded for a fully upended MP and the MP halfway the water depth. For the fully upended MP, only the maximum offlead is exceeded, and only at the spectral peak period of 7.2 seconds. A peak in the displacement and load RAOs of the MP is visible around 6 seconds (Table 7), which explains the increase in response for the smaller T_p in the range of $5.0 - 7.2$ seconds. For the MP halfway the water depth, the offlead is limiting at first, after that the sidelead, and finally the DUF for the pile gripper and the DAF for the crane tip. The displacement and loads RAOs of the monopile are the largest in the range of $12 - 15$

seconds, which explains the increase in response at these larger spectral peak periods. The MP 3 metres above seabed does not exceed the operational limits, similarly to the side installation. The load and displacement RAOs of the monopile are at a maximum around 21 seconds, which is outside the range of the spectral peak periods.

It is observed that similarly to the side installation sequence, the MP halfway the water depth exceeds the most limits, but only for larger T_p. This observation corresponds with the natural period of the double pendulum of 12.8 seconds in combination with the peak of RAOs of the MP and the displacement RAOs of the vessel for heave and pitch (Table 6). The vessel RAO is negligible for roll for head waves, which is the case for stern installation.

The operational limits during upending are presented in Table 8. Only the sidelead is exceeded at 12.8 seconds, which is the only case without a limiting the offlead. For stern installation, the offlead is restricted due to the position of pile gripper ring and the MP placed longitudinally in the centre line. However, a sidelead is possible, which explains the exceedence for the largest simulated H_s for the upended MP. The loading condition with the horizontally placed MP complies for every key indicator.

Table 10: Operability with a maximum off- and sidelead of 3.5°, maximum crane tip DAF of 1.15, crane tip DUF of 1 and pile gripper DUF for x- and y-direction of 1 for range of T_p between 5.0 and 15.0 seconds for a fully upended 2XL MP, a 2XL MP halfway the water depth, and 2XL MP 3 metres above seabed for stern installation

Stern installation		H_s = 2 m	H_s = 3 m	H_s = 2 m	H_s = 3 m	H_s = 2 m	H_s = 3 m
		Fully upended		*Halfway water depth*		*3 m above seabed*	
Crane tip	Sidelead [°]	✓	✓	>9.4 s	>9.4 s	✓	✓
	Offlead [°]	✓	At 7.2 s	>8.3 s	>8.3 s	✓	✓
	DAF [-]	✓	✓	✓	At 11.7, 12.8 s	✓	✓
	DUF [-]	✓	✓	✓	✓	✓	✓
Pile gripper	DUF_x [-]	✓	✓	> 10.6 s	> 9.4 s	✓	✓
	DUF_y [-]	✓	✓	✓	>11.7 s	✓	✓

Comparison side and stern installation

The 5 loading conditions of side and stern installation differ from the wave direction and the position of the monopile compared to the vessel. Other than that, the loading conditions are analogous and this is particularly visible during the lowering stage, for instance for the fully upended MP and the MP halfway the water depth for the offlead as shown in Figure 15. However, the responses during the upending stage show differences due to the change in position of the pile gripper ring and the monopile.

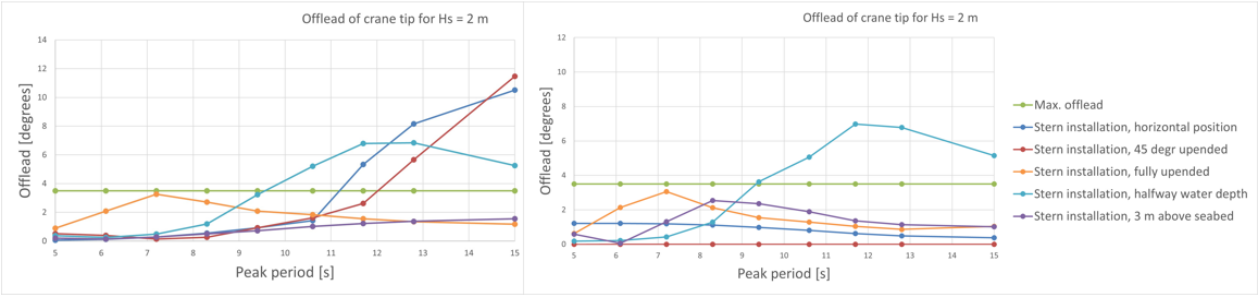

Figure 15: Offlead [°] for H_s = 2 metres for respectively side and stern installation with a maximum allowable limit of 3.5 °

Upending stage: The off- and sidelead are the key indicators that are exceeding the maximum allowable limits during upending. The DAF and DUF of the crane tip are not exceeding limits for both installation methods, since the monopile also partly rests on a cradle. During upending the offlead is not exceeding the allowable offlead, however for the side installation it happens. For stern installation, the monopile is placed in the centre line of the vessel. The pile gripper constrains the

behaviour of the monopile so the offlead for stern installation is smaller during upending than for side installation. During side installation, chaotic double pendulum behaviour occurs when the monopile is in horizontal position, when the spectral peak period corresponds with natural period of the vessel.

Lowering stage: During the lowering stage, the offlead is governing for every loading condition. The case with the fully upended MP does not exceed the allowable limits for H_s = 2 metres. In addition, the offlead is only exceeded at 7.2 and 8.3 seconds for H_s = 3 metres. The RAOs of the monopile are at its maximum in the range of $5.0 - 8.0$ seconds. The case with the MP halfway the water depth exceeds most limits compared to the other 2 loading conditions during lowering, starting from a T_p of 8.3 seconds for both side and stern installation. The natural frequency of the double pendulum coincides with the RAOs of the vessel and the spectral peak period, resulting in exceedence of operational limits in the range of $12 - 15$ seconds. The sidelead for the MP halfway the water depth is exceeded for a smaller T_p compared to side installation. For both installation methods, the DUF of the pile gripper in x- and y-direction is exceeded. The case with the MP 3 metres above seabed does not exceed the allowable limits for both installation methods. The RAOs of the MP are outside the range of the T_p and the RAOs of the vessel. However, for stern installation, there is a maximum in response for the off- and sidelead visible at 8.3 seconds, and corresponding to that for the DUF of the pile gripper in x- and y-direction. This is still underneath the allowable limits, however, in the vessel RAOs graphs for this loading condition there is a local maximum visible.

DISCUSSION

The results of side and stern installation show a difference in operability during upending: stern installation provides a larger operability window than side installation. The lowering phase shows a comparable operability window for both installation methods. Based on the results, for these applied allowable limits a comparison between two methods during upending and lowering can be made. Additionally, differences in responses between T_p and H_s can be observed from the results. This provides an insight into the performance of different methods and helps to gain understanding of the installation of 2XL monopiles. The operability, however, can change based on maximum allowable limits. This paper only zooms in on the operability of the mission equipment during upending and lowering. Current, directional wave spreading, and slamming are not included in the model. More accurate modelling of the recess in HydroD will provide a more realistic shielding effect for stern installation. Steady-state time-domain simulations are performed, which imply an unrealistic build-up of oscillation. For further research, it is recommended to include current, wave spreading, and slamming to have a more realistic model. Moreover, performing nonstationary simulations of both installation methods would provide a valuable and more realistic insight. Simulations of the monopile hook-up could provide further insight into the operational comparison between side and stern installation methods. Lastly, sudden loss of hook load scenarios are interesting to study in more detail. It is expected that stern installation provides advantages compared to side installation. For stern installation, the vessel will not experience any roll-back since the lifting operation is done at the centre line. For side installation, the roll-back can be severe because of the large amount of anti-heeling ballast.

CONCLUSIONS

Concluding, the offlead is generally governing the operational limits for both side and stern installation except during the upending of the monopile with stern installation. For stern installation, during upending, the sidelead can be governing, due to the longitudinal position of the monopile. During upending, the differences in operational limits between side and stern installation are clearly visible: the offlead is limiting the operation only for side installation and not for stern installation. The operability during upending is larger for stern installation. However, during the lowering stage, both installation sequences show a similar course in the key indicators plotted against the spectral peak periods.

For the fully upended MP, the shorter spectral peak periods are critical due to the maximum in RAOs of the monopile. These periods coincide with the spectral peak periods that have a larger chance of occurring on the North Sea. However, the most critical loading condition is the MP halfway the water depth, the operational limits are most exceeded for both in-

stallation sequences, for T_p in the range of $12.0 - 15.0$ seconds. The spectral peak period coincides with the natural period of the double pendulum system of the crane hook and the monopile, and in addition with the natural period of the vessel for heave, pitch, and roll. On the other hand, these operational limits are exceeded for T_p in the range of $12.0 - 15.0$ seconds, which are long waves which do not occur frequently on the North Sea. When the monopile is almost at the seabed, the operational limits are not limiting the operation for both side and stern installation. The natural period of the monopile is then outside of the range of the spectral peak period and the natural period of the vessel.

Stern installation shows a larger operability window during upending compared to side installation. During the lowering stage, the operability differs per loading condition. For the fully upended monopile, stern installation has a larger operability window based on these allowable limits. The results for the monopile 3 metres above seabed are underneath the allowable limits for both side and stern installation. Considering both the upending and lowering phase of 2XL monopiles from heavy lift crane vessel, stern installation shows promising results in terms of operability.

CONTRIBUTION STATEMENT

A.M. Elzinga: Conceptualization; formal analysis; investigation methodology; project administration; validation; visualization; writing – original draft. **J.D. Stroo:** Conceptualization; resources; supervision; writing - review and editing. **A.A. Kana:** Conceptualization; supervision; writing - review and editing.

ACKNOWLEDGEMENTS

This work was performed as part of the MSc thesis for the lead author (Elzinga, 2024). The thesis was performed in Marine Technology at Delft University of Technology and the authors would like to acknowledge both Delft University of Technology and Ulstein Design and Solutions B.V. for their support of this research.

REFERENCES

Amer, A., Li, L., and Zhu, X. (2022). Dynamic analysis of splash-zone crossing operation for a subsea template. *Sustainable Marine Structures*, 4(2):18–39.

Brans, S., Rinne, A., and Kana, A. (2021). Applying a needs analysis to promote daughter craft for year-round access to far-offshore wind turbines. *High-Performance Marine Vehicles (HIPER '21)*, pages 71–87. September 13-15: Tullamore, Ireland.

Chen, M., Yuan, G., Li, C., Zhang, X., and Li, L. (2022). Dynamic analysis and extreme response evaluation of lifting operation of the offshore wind turbine jacket foundation using a floating crane vessel. *Journal of Marine Science and Engineering*, 10(12).

Dam, M. (2018). Monopile installation assessment: a critical assessment of an oscillating monopile during offshore installation. Master's thesis, Delft University of Technology.

DNV (2021a). *Environmental conditions and environmental loads*. Det Norske Vertias AS, Høvik, Norway.

DNV (2021b). *ST-N001: Marine operations and marine warranty*. Det Norske Veritas AS, Høvik, Norway.

Elzinga, A. (2024). Operational limits of 2xl monopile installation: a comparative analysis between side and stern installation. Master's thesis, Delft University of Technology.

Guachamin-Acero, W., Li, L., Gao, Z., and Moan, T. (2016). Methodology for assessment of the operational limits and operability of marine operations. *Ocean Engineering*, 125:308–327.

Huisman (2021). Technical specification - tmc 270000-5000. Technical report, Huisman Equipment BV.

Inernational Energy Agency (2019). Offshore wind outlook 2019. Technical report, International Energy Agency.

International Maritime Organization (2022). *Code on Intact Stability for all Types of Ships covered by IMO Instruments*. IMO, London, United Kingdom.

Lasdon, L., Waren, A., Jain, A., and Ratner, M. (1978). Design and testing of a generalized reduced gradient code for non-linear programming. *ACM Transactions on Mathematical Software*, 4(1):34–50.

Li, L., Gao, Z., and Moan, T. (2015). Response analysis of a nonstationary lowering operation for an offshore wind turine monopile substructure. *Journal of Offshore Mechanics and Arctic Engineering*, 137(5).

Li, L., Gao, Z., Moan, T., and Ormberg, H. (2014). Analysis of lifting operation of a monopile for an offshore wind turbine considering vessel shielding effects. *Marine Structures*, 39:287–314.

Liu, Y. (2021). Monopile forever: Overcoming the technical boundaries of monopile foundations in deep waters. Master's thesis, Delft University of Technology.

MetOcean Solutions (2020). Mean significant wave height. Avalaible at: https://app.metoceanview.com/hindcast/.

Morison, J., O'Brien, M., Johnson, J., and Schaaf, S. (1950). The force exerted by surface waves on piles. *Journal of Petroleum Technology*, 5:149–154.

Ramírez, L., Fraile, D., Brindley, G., and O'Sullivan, R. (2020). Offshore wind in europe. Technical report, WindEurope.

Sandvik, P. C. (2012). Estimation of extreme response from operations involving transients. *Proceedings of the 2nd Marine Operations Specialty Symposium (MOSS '12)*. August 6-8: Singapore.

Stroo, J. (2022). U-stern cfd in waves rev 04. Presentation, Ulstein Design and Solutions B.V.

Stroo, J. (2023a). Ulstein u-stern foundation installation vessel. Technical report, Ulstein Design and Solutions B.V.

Stroo, J. (2023b). A vessel and method configured to install a foundation structure: Wo 2023/001493 a1.

Ulstein (2019). Future trends offshore wind - rev 2.3. Technical report, Ulstein Design and Solutions B.V.